Biomaterials Science

PAPER

View Article Online
View Journal

Cite this: DOI: 10.1039/c8bm01406j

Bi-enzyme functionalized electro-chemically reduced transparent graphene oxide platform for triglyceride detection†

Sheetal K. Bhardwaj,[a] Ruchika Chauhan,[b] Premlata Yadav,[c] Subhasis Ghosh,[d] Ajit K. Mahapatro,[e] Jay Singh [f] and Tinku Basu*[g]

Recently, increased attention has been drawn to application of graphene and its derivatives for construction of biosensors, since they can be used to rapidly detect the presence of bio-analytes. Present paper establishes the preparation of a unique transducer which relies on toluidine blue (TB), absorbed by electrochemically reduced graphene oxide (ERGO) transparent thin film onto the surface of the indium tin–oxide (ITO) glass electrode. The proposed TB/ERGO/ITO electrode shows excellent reversible electro-chemical properties. The novel platform has been explored to fabricate a triglyceride (TG) biosensor *via* co-immobilizing of lipase (LIP) and glycerol dehydrogenase (GDH) onto TB/ERGO/ITO electrode surface. The fabricated bioelectrode (LIP-GDH/TB/ERGO/ITO) directly oxidizes glycerol (produced by catalytic hydrolysis of tributyrin acting as a model TG) in the presence of GDH. The developed bioelectrode replaces unstable biological irreversible redox mediators NAD^+/NADH, involved in the triglyceride breakdown reaction. NADH causes fouling on the bioelectrode surface in bi-enzymatic estimation of TG and reduces the shelf-life of biosensor. Electrochemical response studies carried out using cyclic voltammetry reveal that the fabricated electrode can detect tributyrin in the range of 50–400 mg dL^{-1} with high sensitivity of 29 pA mg^{-1} dL, low response time of 12 s, long-term stability and a low apparent Michaelis–Menten constant (K_m^{app}) of 0.18 mM, indicating high enzyme affinity of LIP-GDH/TB/ERGO/ITO bioelectrode towards tributyrin. Furthermore, this modified bioelectrode has been explored for estimation of TG with negligible interference in human serum samples. The proposed bi-enzymatic bioelectrode for TG analysis offers an efficient and novel interface for application of graphene and its derivatives in the field of bioelectronic devices.

Received 2nd November 2018,
Accepted 6th January 2019

DOI: 10.1039/c8bm01406j

rsc.li/biomaterials-science

Introduction

Triglyceride (TG), a component of very-low-density lipoproteins (VLDLs), plays an essential role in human metabolism as an energy source and helps to transport dietary fat.[1] Elevated level of TG in the bloodstream leads to atherosclerosis, causing a risk of heart disease, coronary heart disease (CAD) and hypolipoproteinaemia.[2] The risk of CAD and hyperlipidemia necessitates estimating the amount of triacylglycerols in blood since their high concentration (normal range is 40–160 mg dL^{-1} in men and 35–135 mg dL^{-1} in women) may cause various disorders. Indeed, conventional analytical methods used for TG measurement in blood are accurate and cover the clinical range very precisely, but they are very tedious, time-consum-

[a]Amity Institute of Nanotechnology, Amity University, Noida, Uttar Pradesh 201303, India. E-mail: sheeturo@gmail.com
[b]Amity Institute of Nanotechnology, Amity University, Noida, Uttar Pradesh 201303, India. E-mail: ruchikachauhan@hotmail.com
[c]School of Physical Sciences, Jawaharlal Nehru University, New Delhi 110067, India. E-mail: premlata.yadav@gmail.com
[d]School of Physical Sciences, Jawaharlal Nehru University, New Delhi 110067, India. E-mail: subhasis.ghosh.jnu@gmail.com
[e]Department of Physics and Astrophysics, University of Delhi, New Delhi 110007, India. E-mail: amahapatro@physics.du.ac.in
[f]Department of Chemistry, Institute of Science, Banaras Hindu University, Varanasi 221005, India. E-mail: jaimnnit@gmail.com
[g]Amity Institute of Nanotechnology, Amity University, Noida, Uttar Pradesh 201303, India. E-mail: tbasu@amity.edu

†Electronic supplementary information (ESI) available: Figures and brief notes, including transparency (Fig. S1), reversible nature of ERGO/ITO, TB/ERGO/ITO and LIP-GDH/TB/ERGO/ITO bioelectrodes (Table S1), conventional and proposed scheme of oxidation of glycerol in presence of GDH (Fig. S2), electrochemical studies including control testing of ERGO/ITO electrode (Fig. S3a), electrochemical analysis of TG catalytic decomposition in the presence of LIP and GDH with new proposed enzymatic pathway based on only GDH/TB/ERGO/ITO bio-electrode by exposing to various concentrations of glycerol (Fig. S3b), recorded CV scans for low concentration of TG and effect of pH on LIP-GDH/TB/ERGO/ITO bio-electrode (Fig. S4), shelf-life study of ERGO/ITO and LIP-GDH/TB/ERGO/ITO bioelectrode as well as effect of response of LIP-GDH/TB/ERGO/ITO bioelectrode by applying consecutive cycle of CV (Fig. S5). See DOI: 10.1039/c8bm01406j

ing, and require expensive reagents, long sample preparation, costly equipment, and skilled manpower.[3] Assuredly, enzyme-based biosensors are gaining popularity owing to their smart, simple, sensitive, rapid response and online monitoring strategy.[4] TG sensing follows two pathways: (i) single step which involves monitoring of change in pH produced by hydrolysis of TG by lipase (LIP) and (ii) multi step process which involves hydrolysis of TG by LIP and subsequent quantification of H_2O_2, produced by oxidation of glycerol by multi enzyme or single enzyme glycerol dehydrogenase (GDH). One carbon atom thick graphene nanosheets should be constructed using the best materials as it offers outstanding catalytic ability, originating from a vast π electron network.[5] However, because of restriction of high quality bulk graphene production, it is found to have very limited application in real life. Therefore, reduced graphene oxide (RGO) is becoming progressively more common in electronic and biosensing applications than pure graphene.[6] RGO can be prepared by chemical, electrochemical, thermal and bacterial reduction of graphene oxide (GO). Motivated by the advantages of electrochemical reduction, such as eco-friendly synthesis, direct film formation, ease of fabrication, and tunability of thickness and electrochemical properties,[7] we have developed a unique stable transparent film of electrochemically reduced graphene oxide (ERGO), covering ITO electrode (ERGO/ITO) at neutral pH, *via* chronoamperometric reduction of GO in water dispersion. The ERGO/ITO electrode exhibits unique electrochemical properties, such as reversibility, stability and high electron transmission rate. The developed surface is explored to design a TG biosensor (LIP/ERGO/ITO) using LIP as a sensing agent. Though, the LIP/ERGO/ITO biosensor for TG detection is simple, sensitive and fast, its pH sensitivity, diagnosed by the presence of uric acid, lactic acid, or ascorbic acid, sometimes causes false response owing to the change in pH of the medium.[8–10,11]

To get rid of the pH shift problem, it is preferable to adopt a multi-step process for detection of TG.[1,12,13] Again, the choice is between oxidation of glycerol by single enzyme (GDH) or multiple enzymes (Glycerol kinase and Glycerol-3-phosphate oxidase). Obviously, the accuracy of a sensing device demands simplicity. Therefore, the most reliable method for the design of a TG biosensor should be based on a bi-enzymatic route, which is hydrolysis of TG by LIP to produce glycerol and fatty acid, and later on, oxidation of glycerol by GDH using NAD^+/NADH as a biological mediator.[14,15] Stumbling blocks in the bi-enzymatic platform comprising LIP and GDH are irreversibility of redox couple (NAD^+/NADH) and high overpotential required for direct oxidation of NADH at a solid electrode surface, causing electrode fouling and eventually leading to poor shelf life of the electrode. Laurinavicius *et al.* have demonstrated the electrochemical determination of TG in the presence of LIP and glycerol dehydrogenase (GDH) on a modified carbon electrode surface in the presence of NADH.[14] They have studied the electrochemical catalysis of NADH oxidation using different redox mediators, such as toluidine Blue O (TB), Nile Blue (NB), or Meldola Blue (MB), and found higher sensitivity with TB and MB. Different approaches, including incorporation of toluidine blue O (TB) and Meldola Blue as redox mediators,[15] iridium nanoparticles, electrophoretically deposited polyaniline, single-walled carbon nanotubes non composite film,[16] *etc*. have been investigated to reduce the over potential for electrochemical catalysis of NADH oxidation. To the best of our knowledge, none of these attempts could achieve reversible oxidation of NADH, which is a major bottleneck towards designing bi-enzymatic TG biosensors. Therefore, it is indeed necessary to replace NAD^+/NADH redox couple by an alternative reversible redox mediator to fabricate a reliable TG biosensor. The pH sensitivity of LIP/ERGO/ITO biosensor upon electrochemical response to tributyrin curbs its practical applications and motivates us to develop a bi-enzymatic TG biosensor with an alternative catalytic pathway in place of NADH/NAD^+.[11] In present investigation, Toluidine blue (TB), a chemical mediator anchored on ERGO/ITO electrode, is explored for construction of bi-enzymatic LIP-GDH/TB/ERGO/ITO bioelectrode to avoid NAD^+/NADH biological mediator. An alternative mechanism involving TB/ERGO/ITO with GDH enzyme is proposed to explain oxidation of glycerol as shown in Fig. 1. Subsequently, an efficient TG measurement in blood samples has established a reliable and successful performance of the proposed biosensor.

Experimental methods

Chemicals and instruments

Sodium nitrate ($NaNO_3$), sulfuric acid (H_2SO_4 (98%)), potassium permanganate ($KMnO_4$), hydrogen peroxide (H_2O_2 (30%)), and hydrochloric acid (HCL) were purchased from Merck, and graphite powder was procured from Alfa-Aser, India. Lipase (LIP) (from Pseudomonas) with specific activity of 48 U mg^{-1}, glycerol dehydrogenase (GDH) (from Cellulomonas) with specific activity of 77 U mg^{-1}, Toluidine Blue (TB), *N*-hydroxysuccinimide (NHS), *N*-ethyl-*N*-(3-dimethylaminopropyl

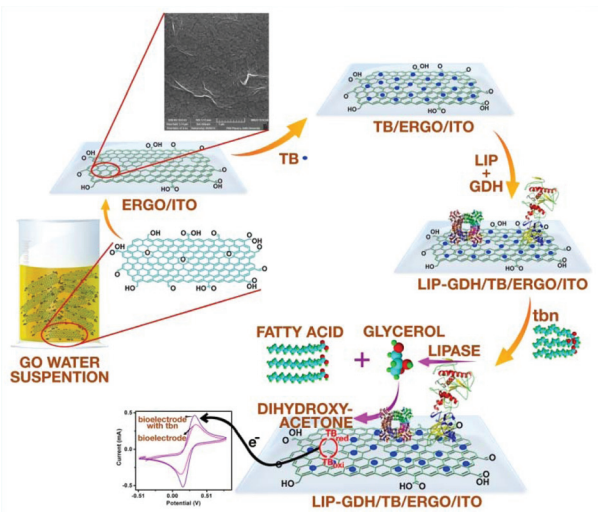

Fig. 1 Schematic presentation of formation of LIP-GDH/TB/ERGO/ITO electrode for TG sensing.

carbodiimide (EDC) and tributyrin (tbn) (a model triglyceride) were procured from Sigma–Aldrich. Electrochemical analysis was conducted on an AutolabPotentiostat/Galvanostat (Model AUT83945, PGSTAT302N) using a three-electrode system with ITO as working electrode, platinum (Pt) wire as an auxiliary electrode and Ag/AgCl as a reference electrode in phosphate buffered saline (PBS, 50 mM, pH 7.4, 0.9% NaCl), containing 5 mM $[Fe(CN)_6]^{3-/4-}$ as a redox probe. Fourier transform infrared spectroscopy (FTIR) analysis was performed using Varian 3100 FTIR spectrophotometer, USA, in the range of 4000–400 cm^{-1}. Raman spectroscopy studies were carried out by Renishaw In using Raman microscope. MIRA3 TESCAN was used for field emission scanning electron microscopy (FE-SEM) analysis.

Preparation of stock solutions

Solutions of LIP (48 U mg^{-1}) and GDH (77 U mg^{-1}) were freshly prepared in PBS (50 mM, pH 7.0). A stock solution of tributyrin was prepared in ethanol and stored at 4 °C. This stock solution was further diluted to prepare different concentrations of the analyte (tributyrin). Solutions of TB (0.1%), EDC (0.4 M) and NHS (0.1 M) were prepared freshly in deionized water.

Fabrication of electrochemically reduced graphene oxide (ERGO) film on ITO electrode

GO was synthesized by modified Hummer's process.[17] The ITO electrodes were cleaned with DI water and acetone. The GO suspension (1 mg mL^{-1}) was reduced on pre-cleaned ITO surface with application of a constant potential at neutral pH (PBS buffer, 50 mM, 0.9% NaCl, pH 7.0) *via* chronoamperometric technique using a three-electrode system with ITO as a working electrode, platinum (Pt) wire as an auxiliary electrode and Ag/AgCl as a reference electrode.[11]

Preparation of TG bioelectrode (LIP-GDH/TB/ERGO/ITO)

The ERGO/ITO electrode was immersed into 0.1% aqueous solution of TB for about 12 h followed by rinsing with water to fabricate TB/ERGO/ITO electrode. After the modification of electrode surface, LIP and GDH were covalently attached to TB/ERGO/ITO electrode *via* carbodiimide chemistry to prepare LIP-GDH/TB/ERGO/ITO bioelectrode. For co-immobilization of enzymes, optimal binding was achieved when 3 : 1 ratio of LIP and GDH, *i.e.* 30 μL solution of LIP (1 mg mL^{-1}) and 10 μL solution of GDH (1 mg mL^{-1}), mixed with 0.4 M EDC and 0.1 M NHS, was added dropwise onto 0.25 cm^2 of TB/ERGO/ITO electrode and kept in a humid chamber for 4 h. Thus fabricated bioelectrode (LIP-GDH/TB/ERGO/ITO) was then washed with PBS solution (50 mM, 0.9% NaCl, pH 7.0) containing 0.05% Tween 20 to remove any unbound enzymes. The LIP-GDH/TB/ERGO /ITO bio-electrodes were refrigerated at 4 °C when not in use.

Study of kinetic properties

Various kinetic properties of LIP-GDH/TB/ERGO/ITO bio-electrode, such as incubation temperature, optimum pH, time of maximum response and tributyrin concentration were examined.

Ethical statement

I testify on behalf of all co-authors that present work was performed in compliance with relevant laws and institutional guidelines. Also, I testify that all authors have been personally and actively involved in substantive work leading to the writing of this manuscript and will hold themselves jointly and individually responsible for its content. We also testify that all human blood serum samples were collected and procedures were performed in accordance with guidelines for care and safety in the nanotechnology laboratory of the university and approved by the ethics committee of Amity university, Noida, India.

Characterization techniques

The ERGO deposited ITO surfaces were characterized for purity and optimized for observation of uniform layers of ERGO flakes using various advanced nanotechnology tools, including Fourier transform infrared (FTIR) spectroscopy (Varian 3100-FTIR spectrophotometer, USA), Raman studies (RenishawInvia Raman microscope, UK), FESEM (MIRA3 TESCAN, Czech Republic), UV-Vis absorption spectroscopy (UV-2401PC spectrophotometer, Shimadzu), high resolution transmission electron microscopy (HRTEM), atomic force microscopy, AFM (Park Systems XE-70, Korea), and cyclic voltammetry (CV), AutolabPotentiostat/Galvanostat Model AUT83945 (PGSTAT302N). Diffraction patterns were acquired by depositing samples directly onto carbon coated Holey grids and imaged using TEM (JEOL-2100F transmission electron microscope, USA) machine, operated at an acceleration voltage of 200 kV.

Detection of tributyrin (a model triglyceride)

A stock solution of tributyrin (as a model triglyceride) in ethanol was diluted to prepare different concentrations of tributyrin. The fabricated TG bioelectrode (LIP-GDH/TB/ERGO/ITO) was exposed to different concentrations of tributyrin. Electrochemical Cyclic Voltammetry (CV) was used for the analysis. CV studies were carried out within applied DC voltage to the working electrode (ranging from −0.4 V to 0.8 V with scan rate of 50 mV s^{-1}) viaAutolabPotentiostat/Galvanostat using the conventional three-electrode system. LIP-GDH/TB/ERGO/ITO bioelectrode was used as the working electrode, platinum wire (Pt) as the auxiliary electrode, and saturated Ag/AgCl as the reference electrode in PBS (50 mM, pH 7.0, 0.9% NaCl) containing 5 mM $[Fe(CN)_6]^{3-/4-}$ as a redox mediator.

Results and discussion

Structural characterization

FESEM, Raman and FTIR analysis. Fig. 2a and b displays FESEM images of electrode surfaces of ERGO/ITO and LIP-GDH/TB/ERGO/ITO, respectively. FESEM image (Fig. 2a) of

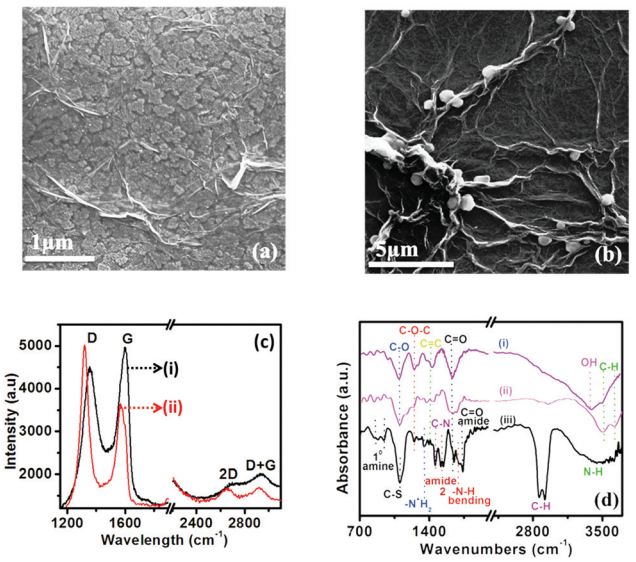

Fig. 2 FESEM images of (a) ERGO/ITO and (b) LIP-GDH/TB/ERGO/ITO surfaces. (c) Raman spectra of ERGO/ITO and GO/ITO surfaces. (d) FTIR spectra of (i) GO/ITO, (ii) ERGO/ITO and (iii) LIP-GDH/TB/ERGO/ITO bioelectrodes.

ERGO/ITO surface demonstrates transparent and uniformly distributed ERGO flakes covering the ITO surface with lifted edges. Here, the folded, lifted edges and the wrinkles are the characteristics of ERGO. Clear ITO surface below the uniformly deposited ERGO film indicates transparency (97.5%; as plotted in Fig. S1 in the ESI†) of FESEM. FESEM image of LIP-GDH/TB/ERGO/ITO bioelectrode (Fig. 2b), captured at a low magnification (5 μm), displays the surface of ERGO flakes with wrinkles and folded edges attached to enzymes. It has been proven that carboxylic (HO–C═O) functional groups are mainly responsible for anchoring enzymes and generally localized at the edges of ERGO flakes.[18,19] Moreover, the presence of globular morphology, seen in Fig. 2b, depicts immobilization of LIP and GDH at the edges of a transparent ERGO film on the surface of LIP-GDH/TB/ERGO/ITO. The crumpled, wrinkled and folded surface of ERGO film provides a large rough surface area for enhanced loading of enzymes.[20]

The prominent D, G, 2D, and D + G bands are present in Raman spectra of the ERGO/ITO and GO/ITO surfaces (Fig. 2c). The peaks corresponding to D and G bands shift from 1352 cm^{-1} to 1320 cm^{-1} and from 1600 cm^{-1} to 1580 cm^{-1}, respectively, from GO/ITO (Fig. 2c, curve i) to ERGO/ITO (Fig. 2c, curve ii). In GO/ITO, the D and G bands with $I_D < I_G$ (as in Fig. 2c) are a measure of fewer in-plane sp^2 domains compared to the sp^3 sites present as a result of extensive oxidation. In ERGO/ITO surface, $I_D > I_G$ suggests the presence of a significant amount of sp^2 sites and structural imperfections upon reduction of GO to ERGO. The ratio I_D/I_G is a measure of the total order of the two-dimensional structure. Here, I_D/I_G values are increased from for GO/ITO to ERGO/ITO.

Fig. 2d depicts FTIR spectra of (i) GO/ITO, (ii) ERGO/ITO and (iii) LIP-GDH/TB/ERGO/ITO bio-electrodes. FTIR spectra of LIP-GDH/TB/ERGO/ITO (Fig. 2d, curve iii) and ERGO/ITO (Fig. 2d, curve ii) electrodes are compared with the spectrum of GO/ITO (Fig. 2d, curve i) by drawing dotted lines at fixed frequencies, representing peak positions and avoiding the frequency range of 2000–2500 cm^{-1} to avoid the CO_2 peak present in all spectra. It has been proven (details are available in ESI†) that partial reduction of oxygen containing functional groups occurs on ERGO/ITO.[11] The appearance of signature peaks in the FTIR spectrum (Fig. 2c, curve iii) of LIP-GDH/TB/ERGO/ITO at 839 cm^{-1} and 943 cm^{-1} corresponds to amine I, 1093 cm^{-1} peak is ascribed to C–S stretching, 1346 cm^{-1} peak is ascribed to –N + (H_2) stretching,[21] and finally, the bands at 1448 cm^{-1} correspond to C–N stretching of aromatic amine, revealing anchoring of TB with ERGO surface of LIP-GDH/TB/ERGO/ITO bioelectrode. Furthermore, the presence of amide II peaks at 1546 cm^{-1} (coupled C–N stretching and C–N bending mode), 1732 cm^{-1} peaks (C═O stretching vibration of amide), and 3277 cm^{-1} peaks (N–H stretching vibration) in FTIR spectra of LIP-GDH/TB/ERGO/ITO (Fig. 2d, curve iii) confirms the successful immobilization of enzymes on TB/ERGO/ITO electrode surface. Additionally, the existence of the bands at 1236 cm^{-1} and 1633 cm^{-1} (Fig. 2d, curve iii) proves retention of epoxides (C–O–C) and carbonyl groups (C═O), confirming the presence of ERGO peaks.

Cyclic voltammetry (CV) and electrochemical impedance spectroscopy (EIS)

As seen in Fig. 3a, CV scans were recorded for (i) ITO, (ii) ERGO/ITO, (iii) TB/ERGO/ITO, and (iv) LIP-GDH/TB/ERGO/ITO bioelectrodes using a three electrode system mounted in phosphate buffer and PBS (50 mM, pH 7.0, 0.9% NaCl) containing 5 mM $[Fe(CN)_6]^{3-/4-}$. DC voltage, ranging from −0.4 V to 0.8 V with a scan rate (γ) of 50 mV s^{-1} was applied to the working electrode. Fig. 3b depicts Nyquist plots of (i) ITO, (ii) ERGO/ITO, (iii) TB/ERGO/ITO, and (iv) LIP-GDH/TB/ERGO/ITO bioelectrodes in PBS (50 mM, pH 7.0, 0.9% NaCl) containing 5 mM $[Fe(CN)_6]^{3-/4-}$, scanned in the frequency range from 0.01 to 5 × 10^4 Hz at biasing potential of 0 V. Anodic peak current (I_{pa}) values of ITO, ERGO/ITO, TB/ERGO/ITO and LIP-GDH/TB/ERGO/ITO bio-electrodes were recorded at 0.1 mA, 0.29 mA, 0.33 mA, and 0.26 mA. Three-fold increase in I_{pa} value of ERGO/ITO (0.29 mA) electrode from ITO (0.1 mA) (Fig. 3a, curves i and ii) revels electro deposition of highly conductive ERGO film onto ITO surface. A large increase in I_{pa} is ascribed to the enhanced electro active surface area and facile heterogeneous electron transfer ability of ERGO flakes with an extended π network, leading to a large scale redox conversion.[11] Introduction of redox mediator, *i.e.* TB molecules in ERGO/ITO matrix, further facilitates the electron transfer process during the electrochemical reaction, as evidenced by the enhancement in the I_{pa}, *i.e.* 0.33 mA (Fig. 3a, curve iii). TB embedded onto ERGO/ITO matrix also prevents restacking of ERGO sheets on ITO surface.[22] After immobilization of both enzymes (LIP-GDH) on TB/ERGO/ITO electrodes, the magnitude of the I_{pa} (0.26 mA) is found to decrease because of inherent insulating nature of enzyme which acts as a barrier

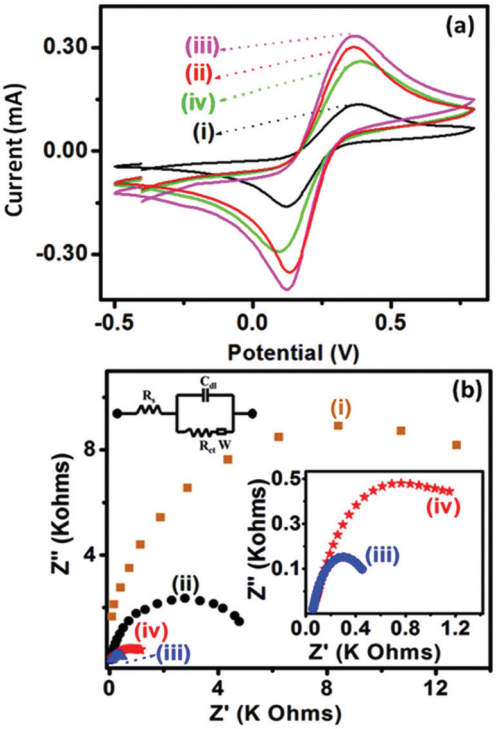

Fig. 3 Cyclic voltammograms of (a) (i) ITO, (ii) ERGO/ITO, (iii) TB/ERGO/ITO, and (iv) LIP-GDH/TB/ERGO/ITO bioelectrodes. (b) Electrochemical impedance spectra of (i) ITO, (ii) ERGO/ITO, (iii) TB/ERGO/ITO and (iv) LIP-GDH/TB/ERGO/ITO bioelectrodes. Inset: Magnified view of impedance spectra of (iii) TB/ERGO/ITO and (iv) LIP-GDH/TB/ERGO/ITO.

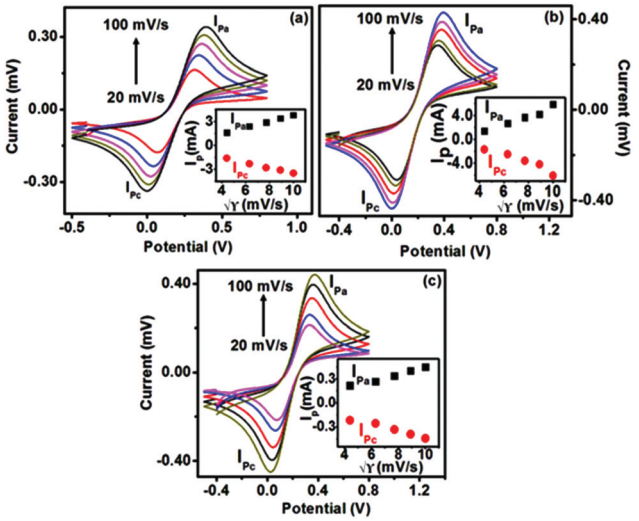

Fig. 4 (a), (b), and (c): CV scans of ERGO/ITO, TB/ERGO/ITO, and LIP-GDH/TB/ERGO/ITO electrodes with increasing scan rate (γ) from 20 to 100 m^{-1}. Inset: plot of magnitude of peak current *vs.* $\sqrt{\gamma}$ (20–100 mV s^{-1}).

for electron transport.[23,24] Interestingly, all electrodes, including bi-enzymatic TG bio-electrodes (LIP-GDH/TB/ERGO/ITO), exhibit reversible electrochemical behaviour (Table S1, described in ESI†). The difference in peak potentials (ΔE, cathodic and anodic) of all the electrodes is almost the same, (0.25 V to 0.27 V) and I_{pa}/I_{pc} ratio remains within 0.8 to 0.9, *i.e.* close to 1 (Table S1†). Interestingly, there is a slight increase in ΔE for the bi-enzymatic bioelectrode, but I_{pa}/I_{pc} ratio increases to 0.9 from 0.8 (TB/ERGO/ITO), confirming reversible nature of the bi-enzymatic bio-electrode. The results of CV studies of ERGO/ITO, TB/ERGO/ITO, and LIP-GDH/TB/ERGO/ITO bio-electrodes with increasing scan rate (γ) from 20 to 100 mV s^{-1} are shown in Fig. 4a–c.

The linear dependence of peak currents and potentials of electrodes ERGO/ITO, TB/ERGO/ITO, and LIP-GDH/TB/ERGO/ITO on γ emphasizes that the redox reaction on electrodes is a diffusion controlled process (detail explanation is given with ESI†). The higher surface concentration of TB/ERGO/ITO (7.06×10^{-8} mol cm^{-2}) than that of ERGO/ITO (6.17×10^{-8} mol cm^{-2}) confirms higher electro active surface area. The values of the heterogeneous electron transfer rate constants (K_s) for the ERGO/ITO, TB/ERGO/ITO, and LIP-GDH/TB/ERGO/ITO electrodes are 0.19 s^{-1}, 0.20 s^{-1} and 0.20 s^{-1}, calculated from the Lavrion model (ESI†), significantly prove fast electron transfer between the immobilized enzymes (LIP and GDH) and the electrode (TB/ERGO/ITO) owing to the presence of TB embedded π–π electron background of ERGO.

The π–π interaction of ERGO and TB, presence of hetero atoms (S, N) and the positive charge in TB make a bridge between the redox cofactor of enzyme, embedded in glycoprotein shell, and the electrode, leading towards an enhancement in heterogeneous electron transfer rate.[15] Fig. 3b shows Nyquist plots recorded for (i) ITO, (ii) ERGO/ITO, (iii) TB/ERGO/ITO, and (iv) LIP-GDH/TB/ERGO/ITO bioelectrode. The semicircular part, seen at higher frequencies, corresponds to the electron transfer-limited process, and its diameter is equal to the charge transfer resistance (R_{ct}), *i.e.* hindrance provided by the electrode material to transfer charge from solution to the electrode, which is correlated to the modification of the surface. The faradaic impedance curve of electrodes has been best fitted with Randles circuit (Fig. 3b). The Randles circuit comprises the resistance of the electrolyte (R_s), in series with the capacitance of the dielectric layer (C_{dl}), and the charge-transfer resistance (R_{ct}), and an additional component Warburg impedance (W). W connects in series with R_{ct}, connected parallel to the capacitance, and accounts for the diffusion of ions from bulk electrolyte to the electrode interface. The magnified view of impedance spectra of TB/ERGO/ITO and LIP-GDH/TB/ERGO/ITO electrodes is shown in inset of Fig. 3b. The values of R_{ct} for bare ITO, ERGO/ITO, TB/ERGO/ITO and LIP-GDH/TB/ERGO/ITO electrodes are 19 kΩ, 6.14 kΩ, 0.13 kΩ and 0.50 kΩ, respectively, reflecting the conductivity of electrodes, given in the following order: TB/ERGO/ITO > LIP-GDH/TB/ERGO/ITO > ERGO/ITO > ITO. The enhanced charge transfer rate of ERGO/ITO is due to the high electron mobility *via* aromatic π conjugated ring structure of the ERGO/ITO electrode, which facilitates diffusion of the negatively charged $[Fe(CN)_6]^{4-/3-}$ ions towards the electrode surface.

Drastic decrease in the R_{ct} value of ERGO/ITO (6.14 KΩ) after TB deposition (0.13 KΩ) is noticed. TB, high electron activity redox species is coupled with ERGO/ITO to decrease the heterogenous charge transfer resistance as seen in the CV study[15,20] (Fig. 3a, curve iii). After the immobilization of enzymes (LIP and GDH) on the surface of TB/ERGO/ITO, the value of R_{ct} is increased to 0.50 kΩ, indicating successful immobilization of LIP and GDH as confirmed by CV scans (Fig. 3b). The insulating nature of the enzymes diminishes conductivity of the bioelectrode (LIP-GDH/TB/ERGO/ITO) as compared to that of TB/ERGO/ITO. The Warburg impedance (W) in the faradaic EIS represents the delay, arising from diffusion of the electroactive species to the electrode, and follows the order ITO > ERGO/ITO > LIP-GDH/TB/ERGO/ITO > TB/ERGO/ITO. The respective values for the order of conductivity of the electrodes are 15.6 kΩ, 1.43 kΩ, 0.03 kΩ, and 0.13 kΩ.[25] The values of C_{dl} in the Randles circuit for ITO, ERGO/ITO, TB/ERGO/ITO and LIP-GDH/TB/ERGO/ITO are 19.6 nF, 2.28 μF, 2.90 μF and 2.66 μF, respectively. The values of C_{dl} exhibit identical order except for LIP-GDH/TB/ERGO/ITO bioelectrode. This phenomenon could have two explanations: (i) double layer capacitance of bioelectrode owing to its complex surface structure and (ii) Randles circuit not being the best fit.

The conventional enzymatic recognition of tributyrin by LIP and GDH enzymes is expressed as follows: hydrolysis of tributyrin by LIP to produce glycerol and fatty acid, followed by the oxidation of glycerol by GDH to produce di-hydroxy acetone in the presence of NAD^+ as a redox mediator, which is a cofactor of GDH (Fig. S2a and 2b†). In the present investigation, an alternative pathway is proposed using embedded TB on ERGO/ITO surface of LIP-GDH/TB/ERGO/ITO bioelectrode to decompose glycerol on the anode in order to replace unstable irreversible NAD^+/NADH. In order to prove the concept, an additional bioelectrode (GDH/TB/ERGO/ITO) was fabricated *via* immobilization of GDH on TB/ERGO/ITO electrode and the following investigations were carried out: control study of the response of TB/ERGO/ITO electrode to glycerol and study of GDH/TB/ERGO/ITO bioelectrode response to glycerol. These studies were conducted in the presence of 100 μL of glycerol of varying concentrations in PBS (50 mM, pH 7.8, 0.9% NaCl) containing 5 mM $[Fe(CN)_6]^{3-/4-}$ at γ of 50 mV s^{-1}. CV studies were carried out to record the response of GDH/TB/ERGO/ITO bioelectrode to glycerol within the applied DC voltage to the working electrode (GDH/TB/ERGO/ITO) ranging from −0.4 V to 0.8 V with scan rate of 50 mV s^{-1} *via* AutolabPotentiostat/Galvanostat, using the conventional three-electrode system. The response of TB/ERGO/ITO electrode and GDH/TB/ERGO/ITO bioelectrode towards glycerol is explained graphically in ESI (Fig. S3a and b†). Except for the positive shift in the anodic potential owing to insulating nature of glycerol, no relationship between the response current and concentration of glycerol was observed in the control study of TB/ERGO/ITO (Fig. S3a(i and ii)†) in the presence of glycerol. On the contrary, the GDH/TB/ERGO/ITO bioelectrode recorded a sequential increase in the concentration of glycerol, depicting recognition of glycerol in the absence of NAD^+/NADH (Fig. S3b†). Detailed results are presented in the ESI.†

The mechanism of oxidation of glycerol in the presence of GDH with the help of TB/ERGO as redox mediator on GDH/TB/ERGO/ITO electrode is depicted in Fig. 5. On the basis of this study, catalytic effect of TB and ERGO on oxidation of glycerol by GDH/TB/ERGO/ITO bio-electrode is explained and the steps of the recognition event are presented. Zinc ion from GDH enzyme coordinates with two successive hydroxyl group of glycerol. The redox mediator TB abstracts H^+ ion, released from glycerol, undergoes reduction and subsequent oxidation by leaving the hydrogen to ERGO. The above concept motivates bi-enzymatic LIP-GDH/TB/ERGO/ITO bio-electrodes to get exposed to increasing concentration of tributyrin solution in PBS (50 mM, pH 7.8, 0.9% NaCl) containing 5 mM $[Fe(CN)_6]^{3-/4-}$ at γ of 50 mV s^{-1}. CV measurements were conducted under the identical electrochemical parameters. Catalytic hydrolysis of tributyrin by LIP and subsequent oxidation of glycerol (Fig. S2†) on LIP-GDH/TB/ERGO/ITO cause an increase in current in the presence of tributyrin, described in eqn (1)–(5):

$$\text{tributyrin} \xrightarrow{\text{LIP}} \text{Glycerol} + \text{Fatty acid} \quad (1)$$

$$\text{Glycerol} \xrightarrow{\text{GDH}} \text{Dihydroxyacetone} + H^+ \quad (2)$$

$$H^+ + \text{TB (Oxid)} \rightarrow \text{TB (Red)} \quad (3)$$

$$\text{TB (Red)} + \text{ERGO (Oxid)} \rightarrow \text{TB (Oxid)} + \text{ERGO (Red)} \quad (4)$$

$$\text{ERGO (Red)} \rightarrow \text{ERGO (Oxid)} + e^- (\text{electron}) \quad (5)$$

The released electron increases the peak current with increasing concentration of tributyrin. Fig. 6a presents a pair of well-defined and symmetric redox peaks of $[Fe(CN)_6]^{3-}$/$[Fe(CN)_6]^{4-}$ on LIP-GDH/TB/ERGO/ITO bioelectrode in presence of various concentration of tributyrin (50–400 mg dL^{-1}). It is important to note that the potential difference (ΔE

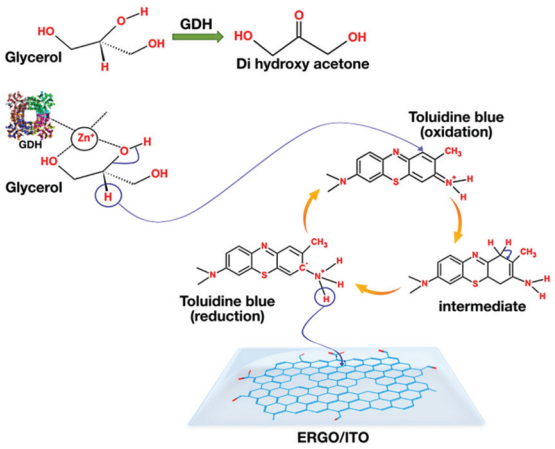

Fig. 5 Scheme of reaction mechanism of oxidation of glycerol in the presence of GDH with the help of TB/ERGO as redox mediator on GDH/TB/ERGO/ITO electrode.

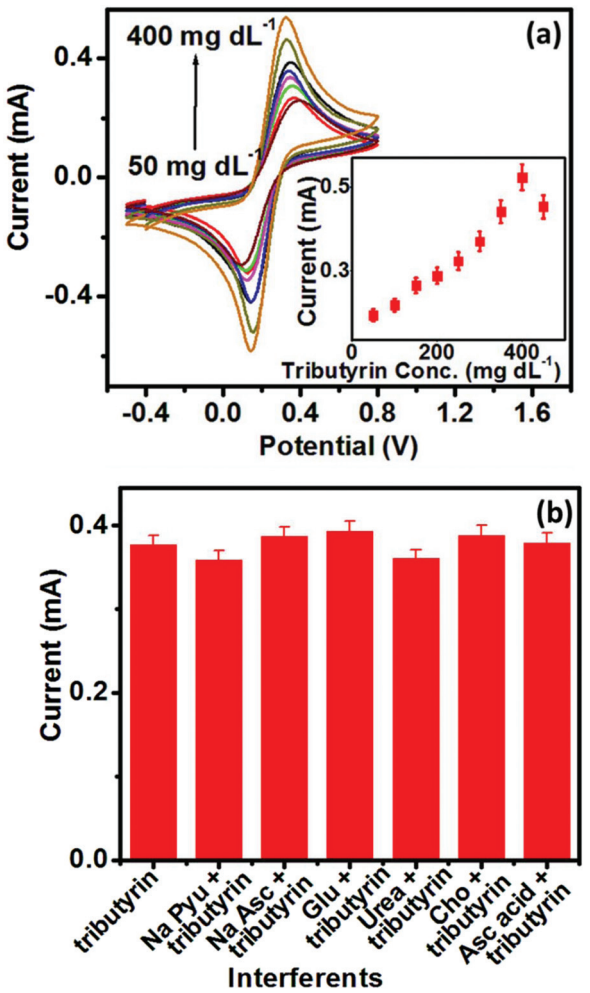

Fig. 6 (a) Response studies of LIP-GDH/TB/ERGO/ITO bioelectrode to varying concentrations of tributyrin within a potential window from −0.5 V to 1.5 V at a scan rate of 50 mV s^{-1}, using conventional three electrode system. Inset: Calibration curve. (b) Plot of the effects of interferents on the response of LIP-GDH/TB/ERGO/ITO bioelectrode.

between E_{pa} and E_{pc}) and peak current ratio (I_{pa}/I_{pc}) of the LIP-GDH/TB/ERGO/ITO bioelectrode in the presence of tributyrin in PBS buffer solution are ≈0.27 V and ≈1, respectively, confirming reversible behaviour of the bioelectrode in the presence of analyte tributyrin.[26]

Response, pH and interference study of LIPLIP-GDH/TB/ERGO/ITO bioelectrode

The response of the LIP-GDH/TB/ERGO/ITO bioelectrode towards tributyrin in PBS containing $[Fe(CN)_6]^{3-}/[Fe(CN)_6]^{4-}$ clearly reveals successful replacement of NAD^+/NADH catalyst by LIP-GDH/TB/ERGO/ITO bioelectrode in the presence of $[Fe(CN)_6]^{3-}/[Fe(CN)_6]^{4-}$. The catalytic effect of LIP-GDH/TB/ERGO/ITO bioelectrode offers a direct transfer of an electron from the active centre of the GDH to TB/ERGO/ITO electrode *via* the π electron networking.[27] Inset of Fig. 6a shows the calibration curve of LIP-GDH/ERGO/TB/ITO bioelectrode for the magnitude of response I_{pa} as a function of tributyrin concentrations at 0.34 V. As the concentration of tributyrin increases from 50 to 400 mg dL^{-1}, I_{pa} increases gradually as shown in Fig. 6a. Slightly increase in the current is observed when the same electrode (LIP-GDH/TB/ERGO/ITO) is exposed to 25 mg dL^{-1} as shown in Fig. S4a.† This constructed bioelectrode can detect tributyrin in the range of 50–400 mg dL^{-1} with a low response time of 12 s. Response time was calculated on the basis of the time taken to reach the optimum current when LIP-GDH/TB/ERGO/ITO bioelectrode was exposed to 150 mg dL^{-1} in the PBS (50 mM, pH 7.8, 0.9% NaCl) containing 5 mM $[Fe(CN)_6]^{3-/4-}$ at the potential of 0.34 V. Each experiment was repeated thrice to confirm the reproducibility of LIP-GDH/TB/ERGO/ITO bioelectrode results. The value of sensitivity, calculated from a linear region of the calibration curve, is 29 pA mg^{-1} dL, with linear regression coefficient (r) and standard deviation (SD) of 0.98 and 1.8, respectively. The equation for the line of regression is given by eqn (6):

$$I_{pc} = 1.2 \times 10^{-4} + (7.6 \times 10^{-7})C_t, \quad (6)$$

where C_t is the concentration of TG (mg dL^{-1}). The apparent Michaelis–Menten kinetic parameter (K_m^{app}) of the enzymatic reaction, which determines the affinity of the enzyme for the bio-analyte, is estimated using Hanes plot, *i.e.* a plot of the reciprocal of current response and the inverse of analyte concentration. The K_m^{app} value for the immobilized enzymes (LIP and GDH) is found to be as 0.18 mM, which is much lower than the previously reported value (2.4 mM, 46 mg dL^{-1}).[28] The low K_m^{app} further signifies that LIP-GDH/TB/ERGO/ITO offers a favourable micro environment for the biochemical interaction of enzymes with the analyte. The effect of pH ranging from 6.5 to 8 on the electrochemical response of LIP-GDH/TB/ERGO/ITO bioelectrode was evaluated in different PBS buffer solutions, containing $[Fe(CN)_6]^{3-/4-}$ and 150 mg dL^{-1} of tributyrin (Fig. S4b†). The optimum response of LIP-GDH/TB/ERGO/ITO bioelectrode is achieved at pH 7.8, as shown in ESI.† Therefore, all experiments were carried out at pH 7.8.

Fig. 6b shows the effects of interferents on the response of LIP-GDH/TB/ERGO/ITO bioelectrode. The study of various interferants of tributyrin detection using LIP-GDH/TB/ERGO/ITO bioelectrode was performed by comparing the I_{pa} of tributyrin exposed LIP-GDH/TB/ERGO/ITO bioelectrode with I_{pa}, recorded for solutions containing 5 mM $[Fe(CN)_6]^{3-/4-}$in PBS (50 mM, pH 7.8, 0.9% NaCl) with various serum contents of urea [(Ur) (1 mM)], glucose [(Glu) (5 mM)], ascorbic acid [(Asc) (0.05 mM)], sodium pyruvate [(Na Pyu) (0.1 mM)], sodium ascorbate [(Na Asc) (0.05 mM)], and cholesterol [(Cho) (5 mM)] at their physiological concentrations. The change in I_{pa} was observed during CV scans of various substances (interferants) in PBS containing 100 μL of 150 mg dL^{-1} of tributyrin solution with 100 μL of interferents in 1 : 1 ratio. In Fig. 6b, the first bar shows I_{pa} obtained in the presence of 150 mg dL^{-1} of tributyrin. The remaining bars show the I_{pa} values corresponding to the mixture of tributyrin (100 mg dL^{-1}) and interferents. The percentage interference (% Int) was calculated using eqn (7)

for various interferents where $I_{\text{tributyrin}}$ is the anodic peak current, obtained in the presence of 150 mg dL^{-1} tributyrin and $\Delta_{\text{Int+tributyrin}}$ is the current obtained for 1 : 1 mixture of tributyrin and interferent.

$$\%I_{\text{int}} = \frac{I_{\text{int+tributyrin}} - I_{\text{tributyrin}}}{I_{\text{tributyrin}}} \times 100 \quad (7)$$

Variation in observed current in the presence of desired interferents (maximum of 5.4%) is due to uric acid. The minimum interference, offered by various acids and urea on the response of LIP-GDH/TB/ERGO/ITO bioelectrode towards recognition of tributyrin, is attributed to the bienzymatic recognition event of a coupled enzyme system of LIP and GDH.

An effort was made to estimate TG concentration using LIP-GDH/TB/ERGO/ITO bioelectrode in human blood serum samples, obtained from optimal diagnostics laboratory, Sarita Vihar, New Delhi, India. During these experiments, the LIP-GDH/TB/ERGO/ITO bioelectrode was dipped in the solution of PBS (50 mM, pH 7.8, 0.9% NaCl) containing 5 mM $[Fe(CN)_6]^{3-/4-}$ and 100 μL of human serum. Response current (I_{pa}) at of 50 mV $s^{-1}$was recorded. The obtained values of TG in serum samples, estimated from the calibration curve (inset of Fig. 6a) using LIP-GDH/ERGO/TB/ITO bioelectrode, are consistent with clinical values (Table 1). Our results suggest that concentration of TG in human serum samples, determined by using the methods developed in the present investigation, is in agreement with the results of spectrophotometric methods in a clinic.

Based on the data in Table 1, it is clear that the proposed LIP-GDH/TB/ERGO/ITO bioelectrode for TG sensing is comparable with other reported TG sensing bioelectrodes. The present TG sensing bioelectrode exhibits a good linear range of 0.5–4.51 mM, which is wider than the previously reported values of 0.56–2.51 for Polyvinyl chloride/Pt[12] and Polyvinyl chloride/Pt.[13] The detection limit (0.18 mM) of presently proposed bioelectrode is comparable with the earlier reported values (0.21, 0.56, 0.37, and 0.22 mM).[12,15,31,32] The biosensing characteristics of the proposed LIP-GDH/TB/ERGO/ITO bioelectrode are comparable with those of other developed TG sensors reported in the literature, along with their important parameters,[29–35] listed in Table S2.†

The shelf-life and reusability of the LIP-GDH/TB/ERGO/ITO bioelectrode are shown in Fig. S5 of the ESI.† The LIP-GDH/TB/ERGO/ITO bioelectrode was exposed to 100 mg dL^{-1} of tributyrine and CV was recoded, but a decrease in the current value was observed after consecutive cycle, as shown in Fig. S5b.† This decrease in current response indicates that the electrodes are not reusable. This is not due to problems with the enzymes; it is a characteristic of electrodes. Final redox reaction, catalyzed by GDH, causes irreversible changes in ERGO as explained by the mechanism (Fig. 5), which gradually changes the characteristic of ERGO platform.

The shelf-lives of both LIP-GDH/TB/ERGO/ITO bioelectrode and ERGO/ITO electrode were evaluated by performing CV measurements in the electrochemical cell, containing tributyrin stock solution as the electrolyte with LIP-GDH/TB/ERGO/ITO as the working electrode at the scan rate of 50 mV s^{-1} and recorded at regular intervals of 7 days by storing the electrodes under refrigerated conditions (4 °C) for future use. The amperometric response currents were measured, and the I_{pa} was plotted for both electrodes in Fig. S6 in the ESI.† The values of I_{pa} of the response currents through the LIP-GDH/TB/ERGO/ITO bioelectrodes and ERGO/ITO electrodes remained almost constant, (up to 90%) recorded at various time intervals for 11 weeks (Fig. S5ii†) and 16 weeks (Fig. S5i†), respectively, and proved protection of electrochemical activity of the enzymes. This observation indicates that the loss in activity of bioelectrode was due to denaturing of the enzymes, not due to instability of ERGO/ITO. Both enzymes were covalently linked with substrate *via* amide linkage (–NHCO) by the covalent reaction between the carboxylic functional group of ERGO and NH_2 of the enzyme, reducing the probability of leaching. The enhanced shelf life of LIP-GDH/TB/ERGO/ITO bioelectrode is a proof of stable biorecognition *via* an alternative pathway through TB/ERGO involving GDH.

Table 1 Analysis of TG content in human blood serum using LIP-GDH/TB/ERGO/ITO

Sample	Values obtained from pathology lab (mg dL^{-1})	Values obtained from LIPGDH/TB/ERGO/ITO electrode (mg dL^{-1})	Percentage error (%)
Sample 1	152	140	5.1
Sample 2	260	245	6.2
Sample 3	305	290	8.5

Conclusions

In summary, electrochemical TG sensor (LIP-GDH/TB/ERGO/ITO) has been developed *via* co-immobilizing of LIP and GDH on the surface of TB modified electrochemically reduced graphene oxide (TB/ERGO/ITO). The transparent ERGO/ITO electrode, prepared in 60 s, possesses a remarkable shelf life of 16 weeks without significant loss in electrochemical activity. The proposed LIP-GDH/TB/ERGO/ITO bioelectrode reveals fast electron transfer with reversible electrochemistry. A stable, reliable biosensing tool was developed based on the improved electrochemical behaviour of TB/ERGO/ITO electrode and explored successfully to replace irreversible unstable NAD^+/NADH biological redox catalyst. The developed TG biosensor, based on LIP-GDH/TB/ERGO/ITO bioelectrode, provides reproducible sensing characteristics with high sensitivity 29 pA mg^{-1} dL, low K_m^{app} value (0.18 mM), TG detection range of 50–400 mg dL^{-1}, and low response time of 12 s. The LIP-GDH/TB/ERGO/ITO bioelectrode has the shelf life of 11 weeks with negligible interference. Considering the reliability, stability, and performance of proposed TG biosensor, it is concluded that LIP-GDH/TB/ERGO/ITO bioelectrode has a promising future in clinical diagnosis. An effort should be made to involve international agencies for speedy commercialization of this bioelectrode.

The bi-enzyme modified transparent ERGO interface offers a novel, efficient and promising platform for other biomedical and nanobioelectronic applications.

Conflicts of interest

There is no conflict to declare.

Acknowledgements

Amity group thanks Dr Ashok Kumar Chauhan (Founder, President, Amity University, Uttar Pradesh) for providing the facilities. We sincerely thank Dr (Mrs) Balvider Shukla, vice chancellor, AUUP., Dr D. K. Avasthi, Director, AINT, AUUP. The authors are thankful to Mr Brijesh Bhardwaj for the graphics.

References

1 W. Liao, C. Liu and T. Chou, *Analyst*, 2008, **133**, 1757.
2 M. Okazaki, N. Komoriya, H. Tomoike, N. Inoue, S. Usui, S. Itoh and S. Hosaki, *J. Chromatogr. B: Biomed. Sci. Appl.*, 1998, **709**, 179.
3 C. S. Pundir and J. Narang, *Int. J. Biol. Macromol.*, 2013, **61**, 379.
4 C. Dhand, P. R. Solanki, K. N. Sood, M. Datta and B. D. Malhotra, *Electrochem. Commun.*, 2009, **11**, 1482.
5 A. K. Geim and K. S. Novoselov, *Nat. Mater.*, 2007, **6**, 183.
6 Q. He, S. Wu, S. Gao, X. Cao, Z. Yin, H. Li and C. P. Zhang, *ACS Nano*, 2011, **6**, 5038.
7 H. Guo, X. Wang, Q. Qian, F. Wang and X. Xia, *ACS Nano*, 2009, **3**, 2653.
8 A. Vijayalakshmi, Y. Tarunashree, B. Baruwati, S. V. Manorama, B. L. Narayana, R. E. C. Johnson and N. M. Rao, *Biosens. Bioelectron.*, 2008, **23**, 1708.
9 C. Wu, X. Liu, Y. Li, X. Du, X. Wang and P. Xu, *Biosens. Bioelectron.*, 2014, **53**, 26.
10 C. Dhand, P. R. Solanki, K. N. Sood, M. Datta and B. D. Malhotra, *Electrochem. Commun.*, 2009, **11**, 1482.
11 S. K. Bhardwaj, P. Yadav, S. Ghosh, T. Basu and A. K. Mahapatro, *ACS Appl. Mater. Interfaces*, 2016, **8**, 24350.
12 C. S. Pundir, S. Singh and J. Narang, *Clin. Biochem.*, 2010, **43**, 467.
13 J. Narang, M. Bhambi and C. S. Pundir, *Anal. Lett.*, 2010, **43**, 1.
14 V. Laurinavicius, B. Kurtinaitiene, V. Gureviciene, L. Boguslavsky, L. Geng and T. Skotheim, *Anal. Chim. Acta*, 1996, **330**, 159.
15 C. Dhand, P. R. Solanki, M. Datta and B. D. Malhotra, *Electroanalysis*, 2010, **22**, 2683.
16 W. Y. Liao, C. C. Liu and T. C. Chou, *Analyst*, 2008, **133**, 1757.
17 W. S. Hummers and R. E. Offeman, *J. Am. Chem. Soc.*, 1958, **80**, 1339.
18 Z. Wang, S. Wu, J. Zhang, P. Chen, G. Yang, X. Zhou, Q. Zhang, Q. Yan and H. Zhang, *Nanoscale Res. Lett.*, 2012, **7**, 161.
19 I. K. Moon, J. Lee, R. S. Ruoff and H. Lee, *Nat. Commun.*, 2010, **1**, 1.
20 P. Sharma, S. K. Tuteja, V. Bhalla, G. Shekhawat, V. P. Dravid and C. R. Suri, *Biosens. Bioelectron.*, 2013, **39**, 99.
21 A. N. S. Rao and V. T. Venkatarangaiah, *J. Electrochem. Sci. Eng.*, 2013, **3**, 167.
22 S. Pei and H. Cheng, *Carbon*, 2011, **50**, 3210.
23 S. K. Bhardwaj, T. Basu and A. K. Mahapatro, *Integr. Ferroelectr.*, 2017, **184**, 92.
24 S. K. Bhardwaj and T. Basu, *Thin Solid Films*, 2018, **645**, 10.
25 J. Song, M. Z. Bazant, J. E. Soc, J. Song and M. Z. Bazant, *J. Electrochem. Soc.*, 2013, **160**, A15.
26 B. Liang, L. Fang, G. Yang, Y. Hu, X. Guo and X. Ye, *Biosens. Bioelectron.*, 2013, **43**, 131.
27 Y. Shao, J. Wang, M. Engelhard, C. Wang and Y. Lin, *J. Mater. Chem.*, 2010, **20**, 743.
28 M. R. Ganjali, F. Faridbod, B. Larijani, H. Rashedi and P. Norouzi, *Int. J. Electrochem. Sci.*, 2010, **5**, 1422.
29 A. K. Gupta, A. Kaushik, P. R. Solanki, C. Dhand, S. Bhansali and B. D. Malhotra, *J. Nanosci. Lett.*, 2014, **4**, 3.
30 R. R. K. Reddy, A. Chadha and E. Bhattacharya, *Biosens. Bioelectron.*, 2001, **16**, 313.
31 P. R. Solanki, C. Dhand, A. Kaushik, A. A. Ansari, K. N. Sood and B. D. Malhotra, *Sens. Actuators, B*, 2009, **141**, 551.
32 J. Narang and C. S. Pundir, *Int. J. Biol. Macromol.*, 2011, **49**, 707.
33 H. Winartasaputra, S. S. Kutan and G. C. Cuilbault, *Anal. Chim.*, 1982, **54**, 1987.
34 D. Compagnone, M. Esti, M. C. Messia, E. Peluso and G. Palleschi, *Biosens. Bioelectron.*, 1998, **13**, 875.
35 M. Bhambi and C. S. Pundir, *Sens. Actuators, B*, 2008, **133**, 251.